

J.P. NARAYAN and A. RAM

## APPLICATION OF FLEXURAL MODELLING TO THE FORMATION OF THE GANGA BASIN OF NORTHERN INDIA

**Abstract.** The rheological properties of the continental crust and upper mantle play a vital role in the development of new sedimentary basins. Rifted sedimentary basins develop during the extension of continental lithosphere. This is inferred from deep seismic data and earthquake seismology. Mathematical modelling of the Ganga basin, situated in the northern part of India, is described in terms of the geometric, thermal and flexural isostatic response of lithospheric extension by planar faulting of the upper-crust and plastic distributed deformation in the lower-crust and mantle. The effect of fault spacing, fault polarity, the amount of extension and the erosion of footwall uplift on crustal structure and basin geometry during both syn-rift and post-rift stages of basin evolution are explored. The purpose of basin simulation is to reconstruct and quantify the geologic evolution of a sedimentary basin in terms of its various parameters. The simulation model integrates all the information regarding the basin to quantitatively assess the hydrocarbon generation potential and quantity of hydrocarbon generated during the basin evolution. The flexural modelling may provide information about formation, migration and accumulation of hydrocarbons in the sedimentary basins. Here initially, a hypothetical lithosphere, with only crust and no mantle is used for modelling the Ganga basin with regard to the Moradabad fault. In the syn-rift modelling of the basin, it is assumed that a planar fault terminates at the seismogenic depth within a fluid of similar density as that of the upper crust. The post-rift flexural isostatic uplift of the lithosphere, responsible for footwall uplift and hangingwall collapse, is calculated. Post-rift crustal thinning of the basin, as well as the thermal field of the lithosphere is determined. The flexural modelling results have revealed that the crustal thinning and thermal gradient generated within the basin during and after lithosphere extension need to be distributed flexurally in order to generate the observed basin depth, geometry and subsidence.

### INTRODUCTION

The flexural cantilever model is a coupled simple shear/pure shear model of the continental lithosphere extension. In this model, footwall and hangingwall blocks are considered to behave as two interacting flexural cantilevers. The response of these cantilevers to the isostatic force produced by extension causes footwall uplift and hangingwall collapse, in the case of normal faulting. In this model, it is assumed that the brittle upper crust deforms by planar faulting, while the ductile lower crust and mantle deforms by distributed pure shear stretching. The flexural strength of the lithosphere may be characterized by its effective elastic thickness, which is the thickness of an unknown perfectly elastic lithospheric plate that would have the same effective flexural rigidity as the lithosphere. The flexural cantilever model assumes flexural (regional) isostasy for the compensation of loads generated by extension, in contrast to the McKenzie model (1978), which assumes Airy isostasy. The effective elastic thickness of the lithosphere during extension is of the order of 2-5 km (Roberts and Yielding, 1991) instead of zero as in the McKenzie model. This low effective elastic thickness has also been supported by Buck (1988) and Kusznir et al. (1991).

The development of rifted sedimentary basins by major crustal faults during extension of

continental lithosphere is supported by deep seismic reflection data (Kusznir and Matthews, 1988) and earthquake seismology. The major basement faults imaged on deep seismic data appear to be restricted to the upper, cool and brittle part of the lithosphere corresponding to the seismogenic layer. The geometry of the basement faults are generally planar, which is supported by earthquake seismology (Jackson, 1987) and elastic dislocation modelling of co-seismic geodetic observations (Stein and Barrientos, 1985). These basement faults generally extend down to 10-15 km depth, corresponding to the base of the seismogenic layer. Jackson and McKenzie (1983), and Kusznir and Park (1987) maintain that beneath this depth deformation gives way to distributed stretching. Extension in the lower lithosphere is achieved by pure shear, and by simple shear in the upper lithosphere (McKenzie, 1978). The continental lithosphere deforms by the combined action of simple and pure shear (Barbier et al., 1986; Kusznir and Park, 1987). The crustal thinning and perturbations to the lithosphere temperature field is caused by simple shear deformation in the upper crust, and pure shear stretching in the lower crust and mantle (Kusznir and Karner, 1985). The above modification leads to a change in the lithosphere density field, which is responsible for subsidence and extensional sedimentary basin formation.

### MATHEMATICAL DESCRIPTION OF THE FLEXURAL CANTILEVER MODEL

Kusznir et al. (1991) assumed that during extensional faulting the footwall and hangingwall blocks behave as two interacting flexural cantilevers, and they developed a mathematical formulation for the flexural cantilever model. The upper crustal surface  $u(x)$  of the model in the absence of gravity for the horizontal extension  $E$  and dip  $\vartheta$  is given by a simple trigonometric relation,

$$\begin{aligned} u(x) &= 0 & x < 0, \\ u(x) &= x \tan \vartheta & 0 < x < E, \\ u(x) &= E \tan \vartheta & x > E. \end{aligned} \quad (1)$$

If the gravity is switched on, the isostatic force (gravity) is given by

$$I_b(x) = -u(x) \rho_c g, \quad (2)$$

and acts on the hangingwall side, where  $\rho_c$  is the density of the crust and  $g$  is the gravitational acceleration.

The buoyancy force acts in the distributed sense because the lower crust and mantle have some finite flexural strength. The flexural isostatic uplift of the lithosphere  $w_b(x)$  in the wavenumber domain is given by

$$W_b(k) = R(k) L_b(k), \quad (3)$$

where  $W_b(k)$  and  $L_b(k)$  are Fourier Transforms of  $w_b(x)$  and  $l_b(x)$  respectively.

Eqn. (3) can also be written as

$$w_b(x) = 1/2\pi \int_{-\infty}^{+\infty} R(k) \left( \int_{-\infty}^{+\infty} l_b(x) e^{-ikx} dx \right) e^{ikx} dk, \quad (4)$$

where  $R(k)$ , the isostatic response function (in  $m^2 s^2/kg$ ) is given by,

$$R(k) = 1 / \left( (\rho_c - \rho_a) g + Dk^4 \right) \quad (5)$$

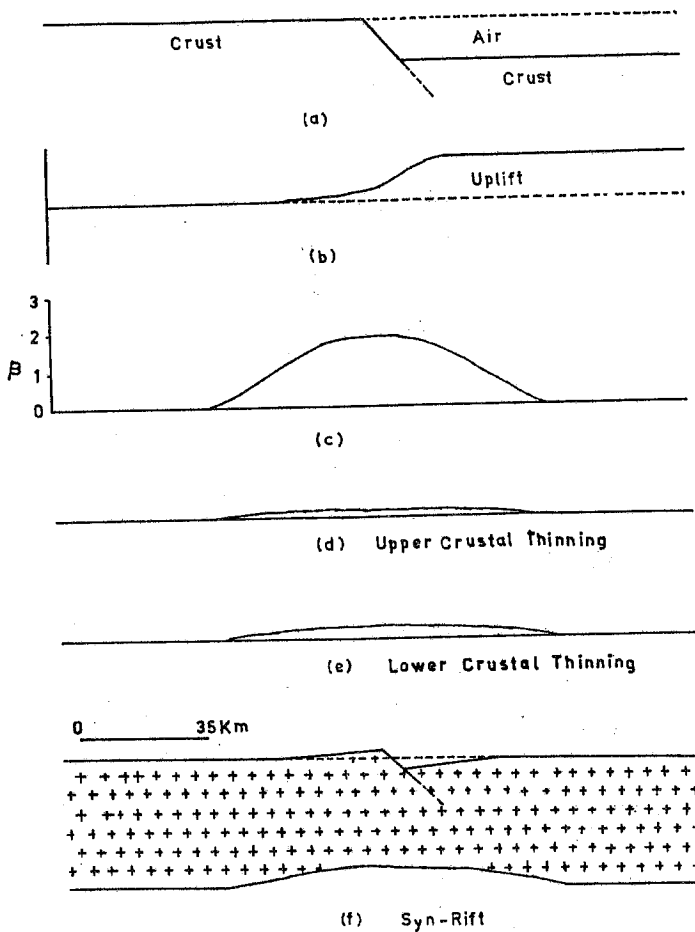


Fig. 1 - a) Geometry of the fault in the absence of gravity, with 10 km horizontal displacement and 45° dip; b) flexural uplift of the lithosphere,  $T_e=3$  km.,  $W=100$  km.; c) Stretching factor  $\beta$  at the Moho; d, e) upper and lower crustal thinning; and f) syn-rift crustal structure and geometry of the basin, predicted by the flexural cantilever model for a single fault.

where  $\rho_a$  is the density of the air,  $k$  is the wavenumber  $=2\pi/\lambda$ , and  $D$ , the flexural rigidity of the lithosphere (in Nm) is given by

$$D = \gamma T_e^3 / (12 (1 - \nu^2)) \tag{6}$$

where  $\gamma$  and  $\nu$  are the Young's modulus and Poisson's ratio respectively, and  $T_e$  is the effective elastic thickness of the lithosphere.

When the flexural uplift  $w_b(x)$  is applied to the upper crustal surface then the post-extensional geometry of the combined upper crustal surface  $s(x)$  is given by

$$s(x) = u(x) + w_b(x). \tag{7}$$

McKenzie (1978) assumed a sinusoidal pure shear stretching factor  $\beta$  to represent the pure shear beneath the brittle ductile transition layer, given as

$$\beta = 1 + C \sin(\pi x/W), \tag{8}$$

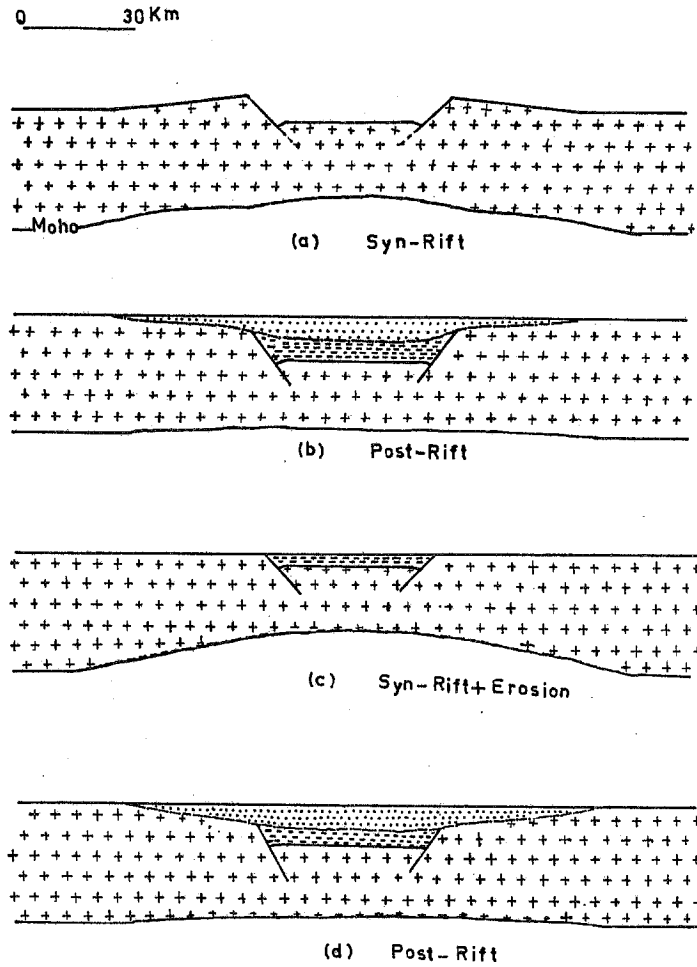


Fig. 2 - a) Syn-rift geometry of the basin predicted by the flexural cantilever model for inward facing faults forming a full graben; b) as a) with sediment-loading and thermal subsidence; c) as a) with uplifted sediments eroded; d) as c) with sediment-loading and thermal subsidence.

where  $W$  is the width of the pure shear region and  $\beta = 1$  represents no extension, for  $W \gg E$ ,  $C = \pi E / 2 (W - E)$ .

The thinning of the lower crust caused by pure shear deformation within lower crust and mantle is given by

$$r(x) = -(d-t) \left( 1 - 1/\beta(x) \right), \quad (9)$$

where  $d$  is the depth of Moho before extension, and  $t$  is the thickness of the brittle upper crust.

Similar set of equations for the loads generated by Moho elevation will be developed.

### LITHOSPHERIC TEMPERATURE FIELD

The pure shear deformation within the lower crust and mantle thins the deeper lithosphere, raises the lithosphere-asthenosphere boundary and increases the geothermal gradient. The syn-rift

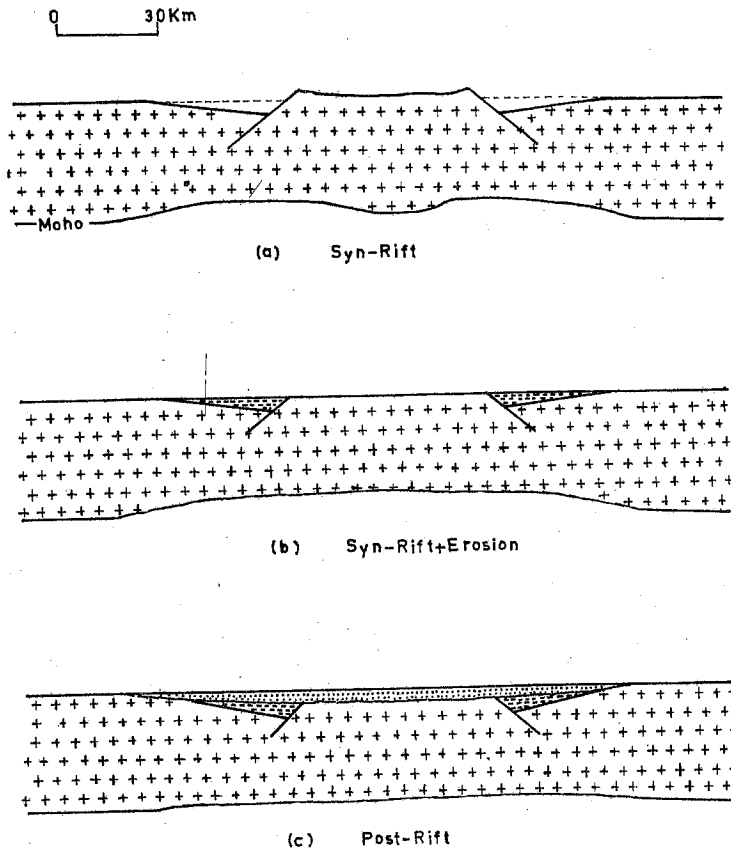


Fig. 3 - a) Syn-rift geometry of the basin predicted by the flexural cantilever model for outward facing faults forming a horst; b) as a) but uplifted sediments eroded; c) as b) with sediment-loading and thermal subsidence.

temperature field given by Kusznir and Egan (1990) is

$$T(z) = z/a T_0 \quad z < a \tag{10}$$

$$T(z) = T_0 \quad z > a,$$

where  $a$  is the lithosphere thickness (125 km) and  $T_0$  is the lithosphere basal temperature (1333°C) (McKenzie, 1978). The geotherm  $T'(z, x)$  after flexural uplift is

$$T'(z, x) = T(z) \beta(x). \tag{11}$$

The post-rift thermal re-equilibrium of the lithosphere temperature field is governed by a differential equation:

$$\partial T / \partial t = K / \rho \sigma \partial^2 T / \partial x^2, \tag{12}$$

where  $K$  and  $\sigma$  are the specific heat and thermal conductivity respectively.

### MODELLING CONFIGURATIONS AND RESULTS

Application of the flexural cantilever model to the geometry and crustal structure of a single

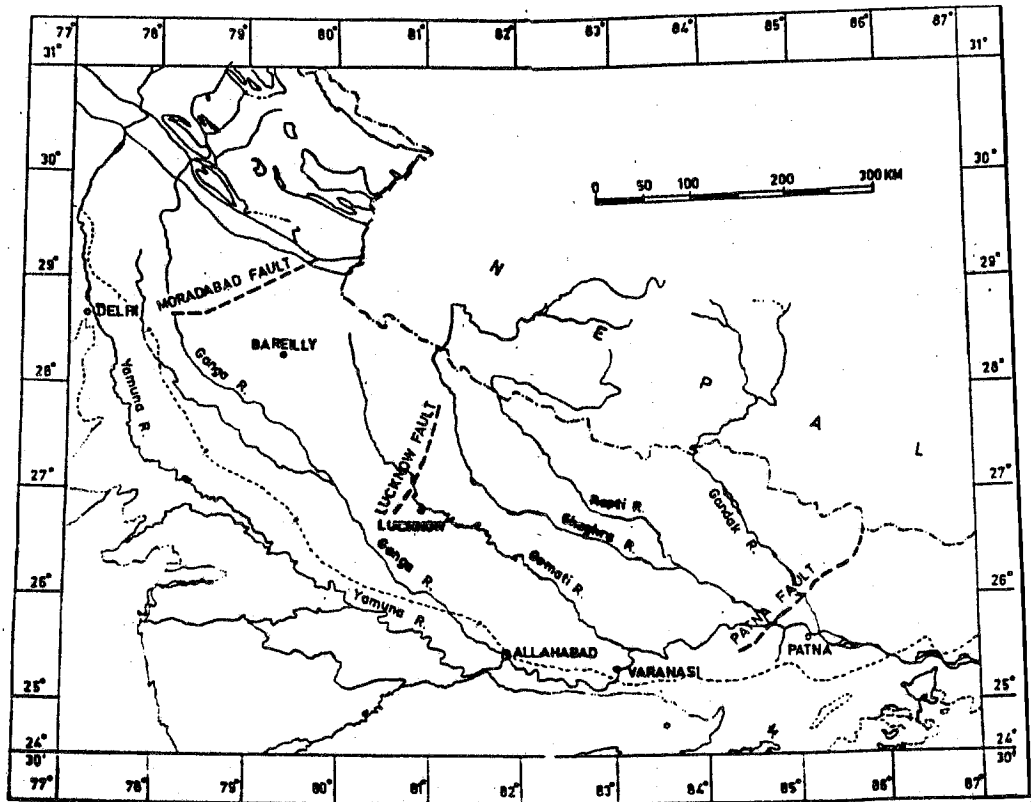


Fig. 4 - Geological map showing the location of the Moradabad fault.

fault with dip  $45^\circ$  is considered. The thickness of the crust, width of the pure shear region ( $W$ ) and effective elastic thickness ( $T_e$ ) are taken as 35 km, 90 km and 3 km respectively. In the absence of gravity, the geometry of this fault obtained from eqn. (1) for an extension ( $E$ ) of 10 km is shown in Fig. 1a. The buoyancy force  $l_b(x)$  is calculated using eqn. (2). In this case, thickness of the upper brittle crust is 11.9 km. The flexural uplift ( $w_b(x)$ ) of the Moho shown in Fig. 1b is obtained in the wavenumber domain using eqn. (4) and incorporating eqns. (5) and (6). The stretching factor  $\beta$  at the Moho is computed using eqn. (8) and is shown in Fig. 1c. Figs. 1d and e illustrate the upper and lower crustal thinning respectively. This thinning is obtained from eqn. (9). The calculated syn-rift response of the lithosphere using eqn. (7) for extension along a single fault is shown in Fig. 1f, prior to sediment filling of the resulting half-graben. The uplift of the Moho is seen under the basin in response to lower crustal thinning by pure-shear and isostatic readjustment of the attenuated lithosphere. The effect of filling the half-graben with sediments and further subsidence due to lithosphere loading has not been incorporated in this case. The stretching factor  $\beta$  reaches a maximum beneath the basin.

Lithosphere extension in a multiple fault system results in interference between the flexural footwall uplift and hangingwall collapse associated with each fault. In Fig. 2a the crustal structure and syn-rift basin geometry for the synthetic faults having opposite polarity are shown. The considered faults are 60 km apart with inclination  $40^\circ$  and they dip towards each other. The extension of the fault and thickness of the upper brittle crust are taken as 15 km each. The response of these faults to the footwall uplift and hangingwall collapse is calculated for the 100 km width of the pure shear region. The resulting basin takes the form of a symmetric full graben (Fig. 2a). The footwalls of the basin bounding faults on both sides of the graben emerge above the ground surface. The Moho shallows substantially under the main basin. Fig. 2b depicts the crustal structure of the basin filled with sediments after 2.5 my of thermal subsidence.

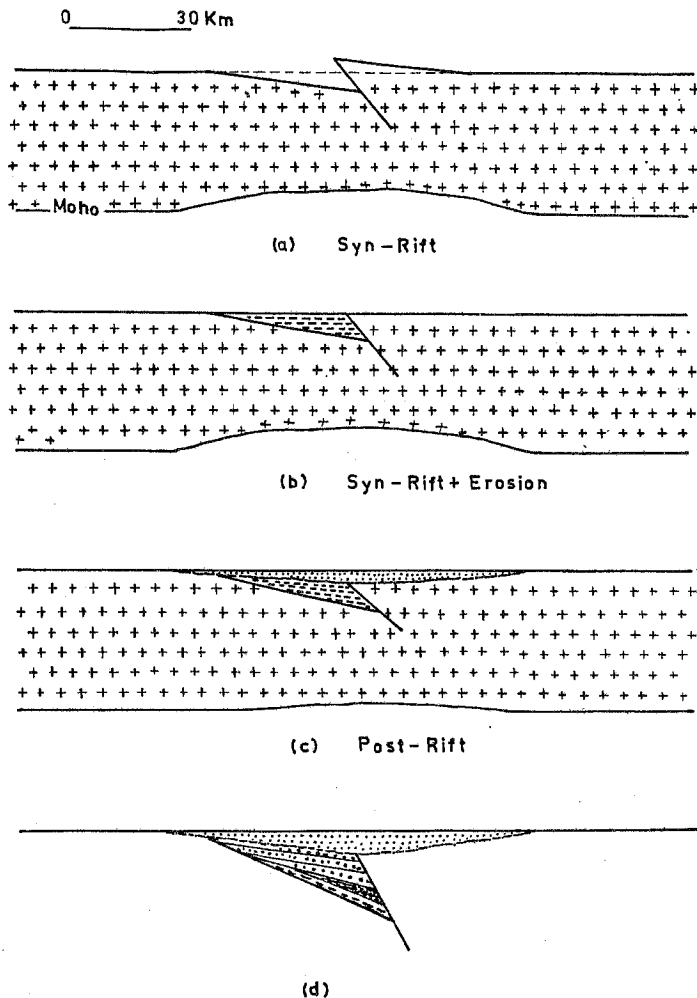


Fig. 5 - a) Syn-rift basin geometry of the Moradabad fault predicted by flexural cantilever model, generating a half graben,  $E=12$  km,  $T_e=4$  km,  $W=90$  km and dip= $40^\circ$ ; b) as a) with sediment filling and erosion of the uplifted portion; c) as b) sediments loading and thermal subsidence; d) vertical exaggeration=2 of the basin geometry.

The differential equation governing the thermal cooling is solved using the central difference finite difference approximation (Mitchell, 1969). Fig. 2c illustrates the structure and geometry of the basin, as well as uplift of the Moho, when only erosion has been allowed for at the same time with a rate of 0.8 mm/year. Similarly, Fig. 2d depicts the post-rift geometry of the basin (Fig. 2c), when thermal subsidence has been allowed for.

In Fig. 3a, the prediction of the flexural cantilever model for lithosphere extension forming a horst involving two adjacent faults with  $40^\circ$  dip is shown. Prior to erosion, the central horst and the footwall of the basin-bounding faults form topographic highs raised above the ground surface. The faults are 50 km apart and each undergoes 12 km extension for 10 km depth of brittle upper crust. In this case, effective elastic thickness and width of the pure shear region are taken as 5 km and 100 km respectively. Fig. 3b depicts the crustal structure and geometry of the basin formed by the horst, when only erosion has been allowed for. The erosion process causes isostatic rebound due to unloading of the lithosphere, as the eroded materials are removed. The resulting uplift allows more erosion to occur. After erosion, the Moho beneath the horst is shallower than in the pre-erosional case. Similarly, Fig. 3c depicts the post-rift geometry

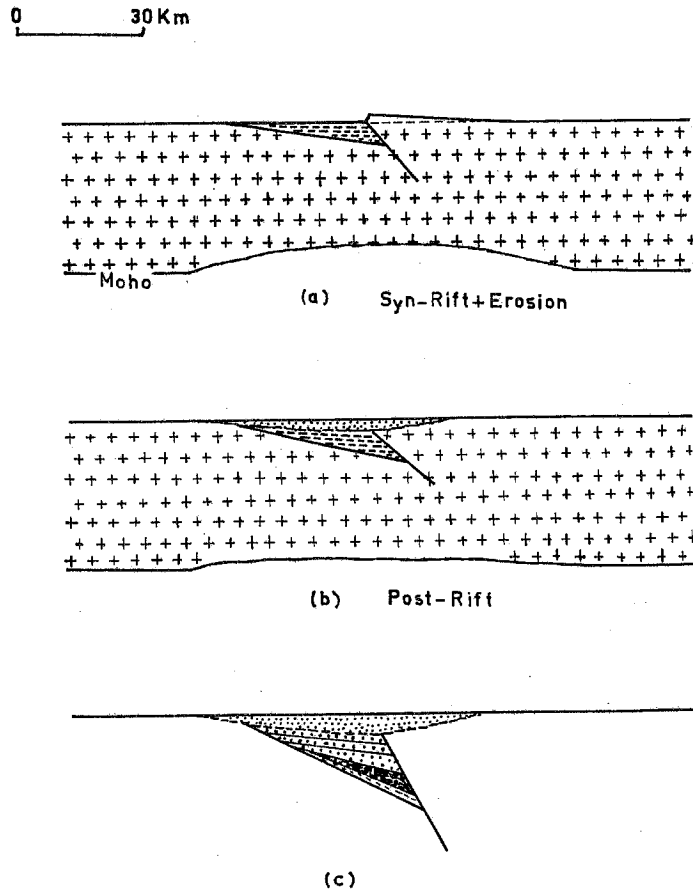


Fig. 6 - a) as Fig. 5a with only sediment filling and no erosion of the uplifted parts; b) as a) sediments loading and thermal subsidence; c) vertical exaggeration=2 of the basin geometry.

and crustal structure of the basin after 2.5 my of thermal subsidence. This Figure illustrates that after subsidence the horst has been converted into a sediment-filled basin and is thickest over the deepest part of the basin.

#### APPLICATION OF THE FLEXURAL CANTILEVER MODEL TO THE FORMATION OF THE GANGA BASIN NEAR THE MORADABAD FAULT

The Ganga basin, one of the major sedimentary basins of India is located on the northern margin of the Indian platform, and occupies an area of about 250,000 sq km falling approximately within Long. 77°E and 88°E and Lat. 24°N and 30°N. The western margin of the basin is limited by a possible extension of the Delhi metasediments to the north, forming a ridge-like feature in the subsurface (Delhi-Hardwar ridge), and the eastern margin is limited by the similar, through broader Monghyr-Saharsa ridge of Satpura metamorphics. The northern part of the Ganga basin is limited by the outermost Siwalik foothills, bounded by a series of reverse faults. Fig. 4 shows the extension of the Ganga basin and location of the Moradabad fault. Along the southern fringes of the basin, Bundelkhand granites/gneisses, and unclassified Precambrian crystalline (Aravalli and Satpura) and Purana sediments (Vindhyan group) are exposed.

The coupled simple-shear and pure-shear model of the extensional sedimentary basin is



applied to the formation of the Ganga basin with reference to the Moradabad fault. The basin has been imaged by seismic reflection profiles, and the stratigraphy of the basin is given by Ahmad and Alam (1978), as shown in Fig. 7. The fault position controlling the localized formation of the basin is shown in Fig. 4. The fault in the model has an inclination of  $40^\circ$  to the horizontal. The thicknesses of the crust, upper brittle crust, and the width of the pure shear region are taken as 35 km, 10 km and 90 km respectively. Since this fault is a thrust fault, opposite flexural uplift occurs in this case; i.e., flexural uplift causes footwall collapse and hangingwall uplift in contrast to the effect of normal faults. The syn-rift geometry and crustal structure of the basin using these parameters, for an effective elastic thickness of 4 km, is shown in Fig. 5a. Fig. 5b depicts the geometry of the Moradabad fault after erosion of the uplifted portion, as well as uplift of the Moho caused by the unloading effect of the erosion. The post-rift geometry and the crustal structure of the basin are shown in Fig. 5c after 2.5 my of thermal subsidence. Fig. 5d depicts the vertical exaggeration of Fig. 5c. Similarly, Fig. 6a illustrates the eroded geometry of the basin. Fig. 6b results when erosion and thermal subsidence are allowed simultaneously. Fig. 6c is the vertical exaggeration of Fig. 6b. A comparison of Figs. 5 and 6 with Fig. 7 shows that the flexural cantilever model applied to the Ganga basin with reference to the Moradabad fault provides close agreement with the observed basin depth and subsidence. The flexural modelling results show that the crustal thinning and thermal gradient generated within the basin during and after lithosphere extension need to be distributed flexurally in order to generate the observed basin depths and geometries. Also, the flexural cantilever model is able to predict crustal structure and sedimentary basin geometry for faults of arbitrary spacing, horizontal displacement and polarity.

## DISCUSSION AND CONCLUSIONS

The coupled simple-shear/pure-shear model developed by Kuszniir et al. (1991), and incorporating the geometric, thermal and flexural consequences of lithosphere extension, is applied to the formation of the extensional sedimentary Ganga basin. The assumed planar geometry of the fault is supported by earthquake seismology data (Jackson, 1987; Stein and Barrientos, 1985). These planar faults generally extend down to 10-15 km, corresponding to the seismogenic layer. Application of the flexural cantilever model to the formation of the Jeanne d'Arc basin, Grand banks and Viking graben of the northern North Sea has been done by Kuszniir et al. (1991). The crustal structure, basin geometry and thickness of the syn- and post-rift sequences of these geological structures have been predicted by the flexural cantilever model. The observed basin geometry and predicted basin geometry from the flexural cantilever model are in good agreement. A similar type of methodology is applied to the formation of the Ganga basin and to other sedimentary basins formed by single and multiple fault systems. The subsurface structure of the Ganga basin (Fig. 7), given by Ahmad and Alam (1978), shows that the Moradabad fault is a reverse fault. The flexural modelling of the reverse fault shows hangingwall uplift and the footwall collapse in contrast to the effect of normal faults (Kuszniir et al., 1991).

The syn-rift geometry and the post-rift geometry of the basin formed by the Moradabad fault are illustrated in Figs. 5a and 5c respectively. Fig. 6b depicts the post-rift structure of the basin, but in this case erosion of the uplifted part is not allowed. A comparison of Figs. 5c and 6b with Fig. 7 shows that the flexural modelling has produced a similar geometry to the Moradabad fault as given by Ahmad and Alam (1978). There are some dissimilarities in the geometry of the fault due to the effect of adjacent faults which were not considered in the modelling. Figs. 1 to 3 indicate that the fundamental building blocks of extensional sedimentary basins are localized rift sub-basins, overlain by a more general thinner post-rift thermal subsidence. The ratio of syn-rift to post-rift thickness is not constant, as predicted by the Mckenzie (1978) model, but is controlled by the locations of faults and their individual displacements and sediment supply. Comparison of Figs. 1 to 3 has also revealed that lateral superposition of stretching for several faults causes thicker post-rift sequences than in the single fault basin. Thus the lithosphere stretching not only leads to mechanical thinning of the crust and mantle, and an increase in geothermal gradient, but also uplifts the lithosphere-asthenosphere boundary and causes a decompression of the underlying asthenosphere. If the stretching and asthenosphere

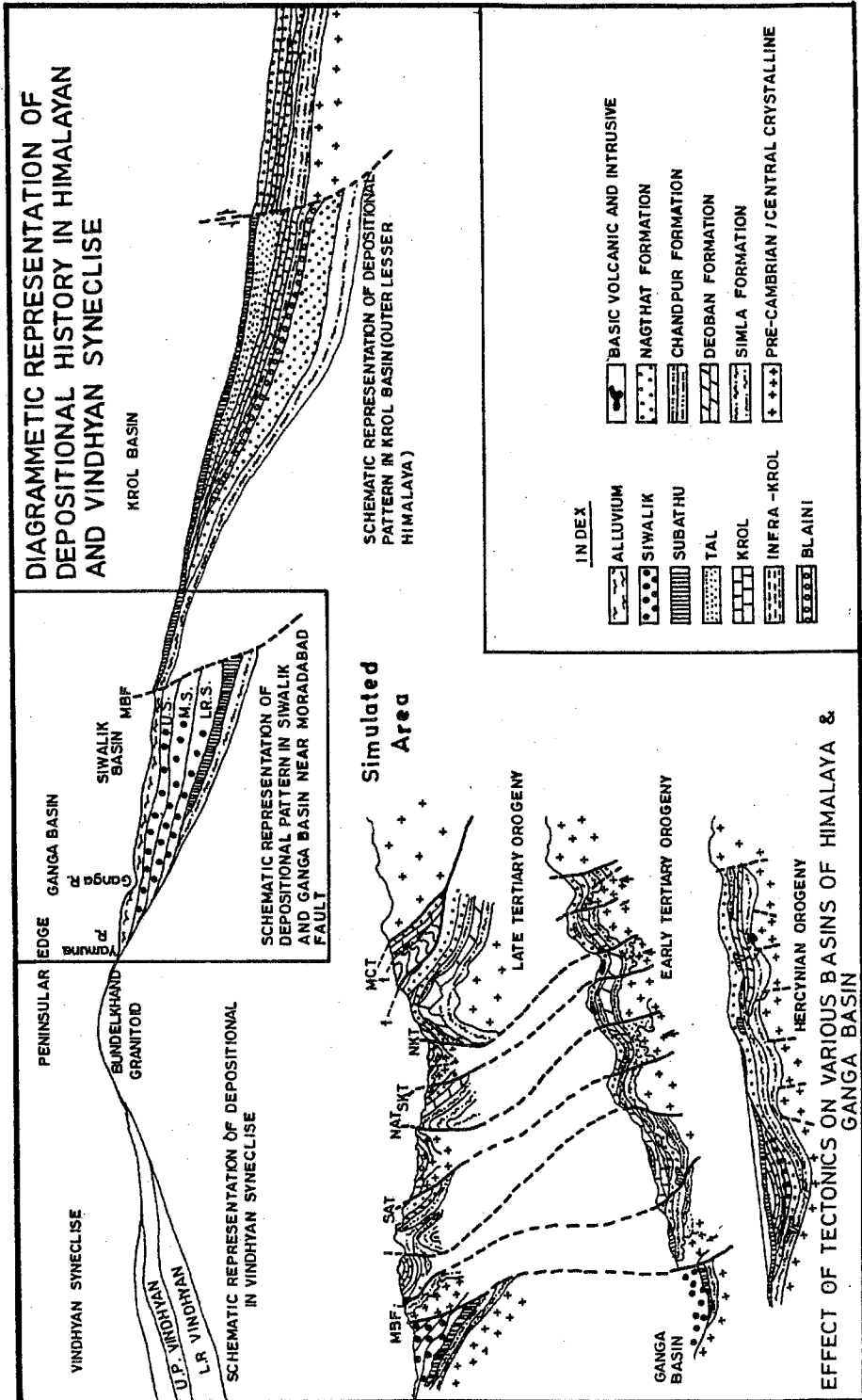


Fig. 7 - Seismic stratigraphy of the Ganga basin near the Moradabad fault (after Ahmad and Alam, 1978).

upwelling is rapid, melting of the upper asthenosphere and lower lithosphere may occur, due to adiabatic changes. Extensive geological and geophysical surveys by the Oil and Natural Gas Commission (ONGC), India, have brought out a clear picture of, and tectonic framework for the Ganga basin. With this information, flexural modelling may provide the most complete record of the thermal history, flexure, orogenies, erosion, and history of the basin evolution. The temperature of the different layers can be obtained. The temperature and amount of organic materials present in the different layers will provide information about the possible formation of hydrocarbon in the basin.

#### REFERENCES

- Ahmad A. and Alam J.M.; 1978: *The Ganga basin, its subsurface sequence, their affinity, sedimentological and tectonic implications*. Himalayan Geology, **8**, 583-608.
- Barbier F., Duverge J. and Le Pichon X.; 1986: *Structure profonde de la marge Nord-Gascogne: Implications sur le mécanisme de rifting et de la formation de la marge continentale*. Bull. Cent. Rech. Expl. prod. Elf-Aquitaine, **10**, 105-121.
- Buck R.W.; 1988: *Flexural rotation of normal faults*. Tectonics, **7**, 959-793.
- Jackson J.A. and McKenzie D.P.; 1983: *The geothermal evolution of normal fault systems*. J. of Struct. Geol., **5**, 471-482.
- Jackson J.A.; 1987: *Active normal faulting and crustal extension*. In: Coward P., Dewey J.F. and Hancock P.L. (eds), *Continental Extensional tectonics*, Geological Society of London, Special Publication, **28**, pp. 3-17.
- Kusznir N.J. and Karner G.D.; 1985: *Dependence of flexural rigidity on the continental lithosphere, rheology and temperature*. Nature, **316**, 138-142.
- Kusznir N.J. and Park R.G.; 1987: *The extensional strength of continental lithosphere: its dependence on geothermal gradient, crustal composition and thickness*. In: Coward P., Dewey J.F. and Hancock P.L. (eds), *Continental Extensional tectonics*, Geological Society of London, Special Publication, **28**, pp. 35-52.
- Kusznir N.J. and Matthews D.H.; 1988: *Deep seismic reflections and deformation mechanisms of the continental lithosphere*. J. Petrology, Special lithosphere issue, 66-87.
- Kusznir N.J. and Egan S.S.; 1990: *Simple shear and pure shear models of extensional sedimentary basin formation, application to the Jeanne d'Arc basin, grand banks of Newfoundland*. In: Tankard A.J. and Balkwill H.R. (eds), *Extensional Tectonics of the North Atlantic Margins*, American Association of Petroleum Geologists Memoir, **46**, pp. 305-322.
- Kusznir N.J., Marsden G. and Egan S.S.; 1991: *A flexural cantilever simple-shear/pure shear model of continental extension*. In: Roberts A.M., Yielding G. and Freeman B. (eds), *The geometry of normal faults*, Geological Society of London, Special Publication, **56**, pp. 41-60.
- McKenzie D.P.; 1978: *Some remarks on the development of sedimentary basins*, Earth and Planet. Sci. Lett., **40**, 25-32.
- Mitchell A.R.; 1969: *Computational methods in partial difference equations*. John Wiley & Sons, New York, 255 pp.
- Roberts A.M. and Yielding G.; 1991: *Deformation around basin margin faults in the North Sea/mid - Norway rift*. In: Roberts A.M., Yielding G. and Freeman B. (eds), *The geometry of normal faults*, Geological Society of London, Special Publication, **56**, pp. 61-78.
- Stein R.S. and Barrientos S.E.; 1985: *Planar high angle faulting in the basin and range: Geodetic analysis of the 1983 borah peak, Idaho Earthquake*. J. Geophys. Res., **90**, 11355-11366.

